Magnon focusing in thin ferromagnetic films

V. Veerakumar and R. E. Camley
Center for Magnetism and Magnetic Nanostructures, Department of Physics, University of Colorado at Colorado Springs, Colorado Springs, Colorado 80933, USA

(Received 9 January 2006; revised manuscript received 2 October 2006; published 1 December 2006)

We study the focusing of bulk and surface spin waves in thin ferromagnetic films. This is done by first solving the implicit dispersion relation obtained from the magnetostatic Maxwell equations. We then obtain slowness surfaces (constant frequency curves in k-space) for the first four bulk modes and one surface mode. The focusing pattern is obtained from the slowness surface by finding the normal to the slowness surface and then evaluating the curvature at each point on the surface. Numerical examples are given for two materials, yttrium iron garnet and iron. It is found that the bulk modes are focused in four to eight distinct directions depending on the frequency and the applied magnetic field. For magnetostatic modes, the surface waves are not focused as strongly as the bulk waves. Also, we study the effect of the exchange interaction on the focusing pattern of both the bulk and surface waves. This is carried out by numerically solving the magnetostatic Maxwell equations along with the equations of motion for the magnetization in thin film to obtain the slowness surface and the focusing pattern. It is found that while the bulk wave focusing is not substantially affected by the exchange interaction, the surface waves now become as strongly focused as the bulk waves. In both cases the focusing direction is tunable with the frequency and applied field.

DOI: 10.1103/PhysRevB.74.214401 PACS number(s): 75.30.Ds, 72.10.Di, 75.70.−i, 85.70.−w

I. INTRODUCTION

There has been substantial interest on the focusing of bulk and surface phonons in elastic solids. Many theoretical[1–4] as well as experimental works[5,6] were carried out and there was excellent agreement between theory and experiment. Phonon focusing can be obtained, for example, by exciting a crystal at typical phonon frequencies using a pulsed laser beam. In an elastically anisotropic crystal, the energy transferred to the crystal by the laser beam travels away, not in circular waves, but in highly focused directions known as caustics. Theoretically, one can find the focusing directions by finding the response function of the material to an oscillating point source and evaluating it a far distance from the source.[3,7]

It is reasonable to consider if other types of modes might exhibit focusing effects. One of the requirements for focusing is that there is some anisotropy in the system so that the group velocity and the phase velocity point in different directions. In the phonon focusing this occurs because of the inherent anisotropy of the crystals. In magnetic materials, one has the additional advantage of being able to tune the degree of anisotropy by applying an external magnetic field, and the resulting focusing patterns are therefore also tunable.

We will first study the focusing behavior of magnetostatic waves. Magnetostatic modes in ferromagnets have been studied extensively in both theory and experiment.[8–10] They propagate in the microwave region and their frequency depends on the magnitude of an applied magnetic field and the properties of the particular ferromagnet. For a thin ferromagnetic film both the volume and surface modes appear as discrete sheets within a band of frequencies. The surface mode has a frequency above the volume modes and is localized on either the top or bottom of the thin film depending on the direction of propagation. Furthermore, for backward volume waves and surface modes the phase and group velocities point in different directions. Thus it makes sense to examine focusing of the magnetostatic modes in thin ferromagnetic films.

Apart from the usual thin film geometry, magnetostatic modes have also been studied in a number of different geometries with finite dimensions using several different approaches including the variational[11] and quantized slab methods.[12] In the case of finite geometries, such as rectangular film, one has to consider the edge effects due to the magnetization pattern which stops abruptly at the edges unlike the infinite plane. This produces end effects which result from the nonuniformity of the dc magnetization field generated by the magnetic poles at the sample ends. The edge effects have the largest effect in the frequency of the lowest mode number and strongly affect the spacing between the modes.[13] On the other hand, the nonuniform demagnetizing field leads to a position dependent wave number for the modes.[13] Recently, a number of analytical and numerical techniques have been used to study modes in finite geometries where exchange is also included.[14–17] In the present paper, we consider a film only with finite thickness and hence we do not include the edge and end effects.

In this paper, we investigate the focusing of surface and backward volume waves (hereafter called as bulk waves) in two different magnetic materials, viz. yttrium iron garnet (YIG) and iron (Fe). This study is carried out by first solving the magnetostatic Maxwell equations in a thin magnetic film. Then the slowness surfaces (constant ω curves in k-space) are obtained for the bulk and surface modes. The focusing pattern is obtained from the slowness surface. We observe that for frequencies near the top of the bulk spin wave band, the bulk modes are focused in eight distinct directions. Bulk modes which occur in the lower frequency portion of the spin wave band are focused into four different directions. Also we find that, for the magnetostatic waves, surface modes are not focused as strongly as the bulk modes. Furthermore, we study the effects of the exchange interaction on the focusing pattern of bulk and surface waves. To do this,

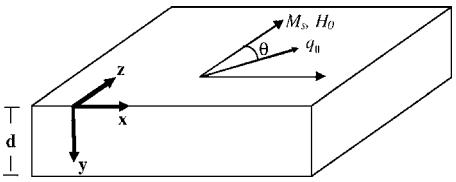

FIG. 1. Geometry of the film for calculating the magnetostatic modes. The applied field and the saturation magnetization are parallel to the surface of the film. The wave vector $q_\parallel$ makes an angle θ with the z direction.

we numerically solve the magnetostatic Maxwell equations along with the equations of motion for the magnetization to obtain the slowness surface and focusing pattern. We find that the focusing patterns of bulk waves are not much affected while the surface waves become focused when exchange is added. Finally in both the cases, the focusing directions are shown to be tunable with frequency and applied field, indicating that this effect might be useful in signal processing devices such as tunable filters and frequency splitters.

The paper is organized as follows. In Sec. II, we obtain the implicit dispersion relation for magnetostatic spin waves. The implicit dispersion relation is solved numerically to obtain the slowness surface for several magnetostatic modes at different frequencies and applied fields for YIG and Fe and the corresponding focusing pattern is discussed in Sec. III. Section IV gives an outline of the calculations including the exchange interaction, and we discuss the exchange effects on the focusing pattern in Sec. V. Finally, in Sec. VI we conclude and discuss possible experimental measurements.

II. THEORY OF DIPOLAR WAVES

The geometry is shown in Fig. 1. The two surfaces of the ferromagnetic film lie parallel to the x-z plane at $y=+d/2$ and $y=-d/2$. An applied magnetic field H_0 is also parallel to the surfaces and in the z direction. The theory of magnetostatic modes in ferromagnetic thin films is well known, and hence we only give a brief outline with the necessary equations for our investigation. The complete theory is given in Ref. 18.

The permeability tensor for a ferromagnetic material is given by[19,20]

$$\vec{\mu}(\omega) = \begin{bmatrix} \mu_1 & -i\mu_2 & 0 \\ i\mu_2 & \mu_1 & 0 \\ 0 & 0 & 1 \end{bmatrix}, \tag{1}$$

where

$$\mu_1 = 1 - 4\pi\left(\frac{\gamma^2 H_0 M_s}{\omega^2 - \gamma^2 H_0^2}\right) \tag{2}$$

and

$$\mu_2 = \left(\frac{4\pi\gamma\omega M_s}{\omega^2 - \gamma^2 H_0^2}\right). \tag{3}$$

In these equations, γ is the gyromagnetic ratio, M_s is the saturation magnetization of the ferromagnet, and ω is the angular frequency.

In the long-wave length limit one can use the magnetostatic form of Maxwell's equations to obtain the Walker equation for the magnetic scalar potential $\phi=\phi(x,y,z,t)$ using the permeability tensor in Eq. (1). The Walker equation for ϕ has a wave solution of the form $\exp(iky)\exp[i(k_x x + k_z z - \omega t)]$, where $k=\pm|q_\parallel|\sqrt{\sin^2\theta+(\cos^2\theta/\mu_1)}$ is the wave vector normal to the film, $k_x=|q_\parallel|\sin\theta$ and $k_z=|q_\parallel|\cos\theta$ are the wave vectors in the x-z plane. Here $q_\parallel=\sqrt{k_x^2+k_z^2}$ and θ is the angle between the z axis and $q_\parallel$ as shown in Fig. 1. The above definition of k corresponds to bulk waves. For surface modes $k=\pm i\alpha$, where $\alpha=\pm|q_\parallel|\sqrt{\sin^2\theta+(\cos^2\theta/\mu_1)}$ and outside the film $k=\pm i|q_\parallel|$. Here θ is the angle between $q_\parallel$ and the x-axis. For proper decay in each region, one can write $k=-i|q_\parallel|$ for $y<-d/2$ and $k=i|q_\parallel|$ for $y>d/2$. Using these definitions, the potentials in each region can be determined. Following this, the boundary conditions which require that the potentials and the normal components of **B** should be continuous at $y=\pm d/2$ can be applied to obtain the following dispersion relation:

$$(\kappa_1 - |q_\parallel|)(\kappa_2 + |q_\parallel|)\exp(\alpha d) - (\kappa_1 + |q_\parallel|)(\kappa_2 - |q_\parallel|)\exp(-\alpha d) = 0, \tag{4}$$

where $\kappa_1=\mu_2 k_x - \alpha\mu_1$ and $\kappa_2=\mu_2 k_x + \alpha\mu_1$. The specific dispersion relation for the volume and surface modes can be easily written from Eq. (4).

Detailed theoretical calculations for the focusing of phonons and magnetoplasmon polaritons[21] have already been carried out. We summarize the key behaviors as follows. One starts by finding constant-frequency curves in the k_x and k_z plane. Such curves are known as "slowness surfaces." The focusing pattern is then found by traveling around the slowness surface and at each point calculating the normal to the surface. The normal indicates the direction of the energy flow. The magnitude of the energy sent in that direction is proportional to $1/a^{1/2}$, where a is the curvature of the slowness surface at a given point. When the curvature is zero, one finds a "caustic" in that the power flow diverges. However, even without a caustic, one can find substantial focusing of the energy as we shall see in Sec. III.

III. NUMERICAL RESULTS AND DISCUSSION

We have solved Eq. (4) numerically for two different ferromagnetic materials, viz. YIG and Fe for different magnitude of applied fields. The bulk frequency ranges from γH_0 to $\gamma\sqrt{H_0(H_0+4\pi M_s)}$. To give a sense of typical numerical ranges, the M_s values, the bulk mode frequency range, and the surface mode frequency in the limit $k_x d\to\infty$ for YIG and Fe are given in Table I for different applied fields.

We begin our study of focusing by examining bulk modes in YIG. Figure 2 shows the slowness surfaces and focusing patterns for the first bulk mode in a 1-μm thick YIG film

TABLE I. Magnetization saturation values and frequency ranges for the magnetostatic bulk and surface modes in YIG and Fe for different magnitudes of applied field.

		H_0=1 kOe		H_0=1.2 kOe		H_0=1.4 kOe	
Material	M_s value (G)	Frequency range for bulk modes (GHz)	Surface mode frequency (GHz)	Frequency range for bulk modes (GHz)	Surface mode frequency (GHz)	Frequency range for bulk modes (GHz)	Surface mode frequency (GHz)
YIG	1.3×10^2	2.8–4.6	5.2	3.4–5.2	5.7	4.0–5.9	6.3
Fe	1.7×10^3	2.8–13.5	33.5	3.4–14.9	34.0	4.0–16.1	34.6

with an applied field of 1 kOe and at three different frequencies. At the lowest frequency, the slowness surface extends only over a small portion of k-space. In Fig. 2(a) the curvature of the slowness surface always has the same sign, so there is no true focusing of energy onto a caustic. Nonetheless, the outgoing energy from the point source does leave primarily in four particular directions because the curvature of the slowness surface varies at different points in k-space. Figure 2(b) shows a very different situation found at higher frequency. Here the curvature of the slowness surface goes to zero at several points and one finds a substantially different pattern with the energy focused along eight true caustics. [Note the scale difference between the focusing patterns in Figs. 2(a) and 2(b).] This is a general pattern that we find in our results, i.e., the number of caustics is larger when ω is in the upper portion of the bulk spin wave spectrum. At higher frequencies, Fig. 2(c) the energy is again focused into eight caustics, but the directions are substantially different. Thus this system can be used to separate signals of different frequencies and has potential as a signal processing device.

Figure 3 shows how the slowness surfaces and the focusing pattern changes when the external field is varied and the frequency held at a single value of 4.5 GHz. In Fig. 3(a), where the field is 1 kOe, we again see focusing into eight caustics. As the field is increased the focusing directions change and at the field of 1.4 kOe there are no true caustics, but some weak focusing remains. [Again, note the different scale between Figs. 3(b) and 3(c)].

This behavior is consistent with our earlier results. As the field is increased, the bulk spin wave band is moved to higher frequencies. Thus the fixed frequency of 4.5 GHz is near the top of the bulk spin wave band at low fields, but moves toward the bottom of the band as the field increased. Again, true focusing along a caustic disappears as the frequency approaches the bottom of the spin wave band.

As is well-known from phonon focusing studies, both bulk and surface modes can exhibit focusing. In Fig. 4 we show the slowness surface and the focusing pattern for the surface mode in YIG. It is well-known that the magnetostatic surface mode in a thin film is nonreciprocal in the sense that the wave is localized at the upper surface of the film for propagation from right to left across the magnetic field and is localized at the bottom surface for propagation in the opposite direction. Because of this we have drawn to slowness surface and focusing pattern for $k_x>0$ to represent the results that might be seen on the upper surface of the film.

It is easily seen that the curvature of the slowness surface for the surface mode is never zero. Thus there are no true caustics for surface mode focusing. However, the curvature is not constant over the slowness surface, so substantially

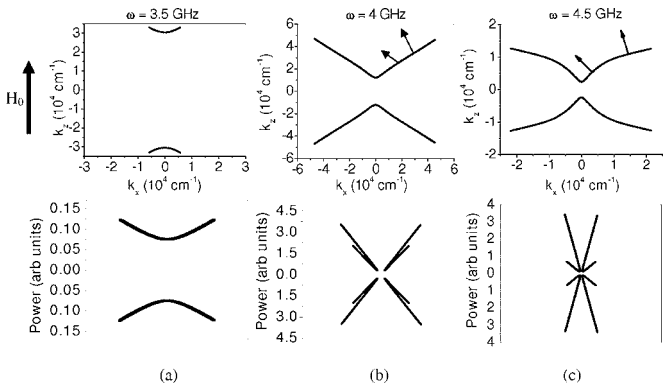

FIG. 2. The upper panel shows the slowness surface and the lower one is the focusing pattern for the lowest bulk mode in YIG with an applied field of 1 kOe at (a) 3.5 GHz, (b) 4 GHz, and (c) 4.5 GHz. The arrows on the slowness surface in (c) show the normals to the slowness surface at some of the points where the curvature is zero.

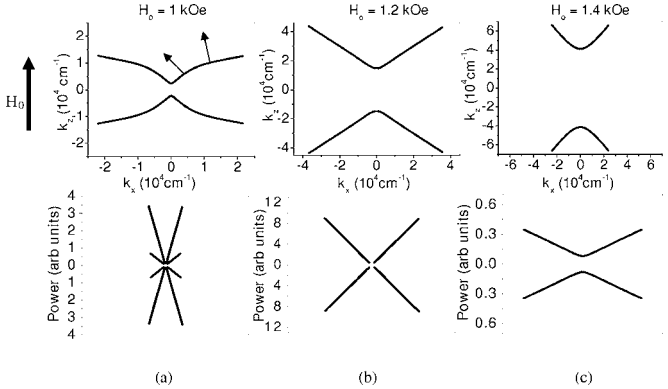

FIG. 3. The upper panel shows the slowness surface for the lowest bulk mode in YIG at a frequency of 4.5 GHz with an applied field of (a) 1 kOe, (b) 1.2 kOe, and (c) 1.4 kOe. The lower panels show the resulting focusing pattern in a polar format. The arrows on the slowness surface in (a) show the normals to the slowness surface at some of the points where the curvature is zero.

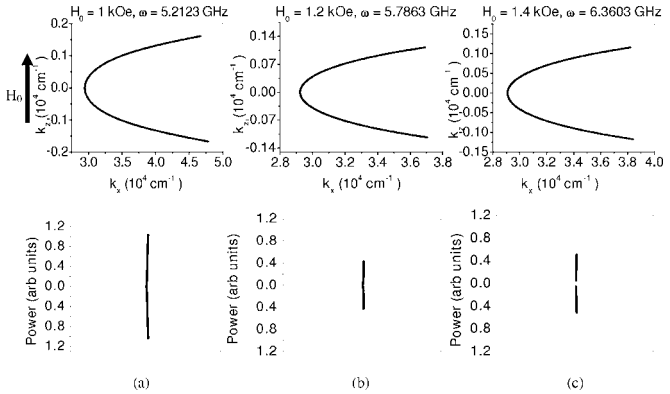

FIG. 4. The upper panel shows the slowness surface and the lower one is the focusing pattern for the surface modes in YIG (a) H_0=1 kOe, ω=5.2123 GHz, (b) H_0=1.2 kOe, ω=5.7863 GHz, and (c) H_0=1.4 kOe, ω=6.3603 GHz.

more energy is sent out in some particular directions. The focusing directions for the surface mode are also tunable with an external field, but substantial changes in field produce only relatively modest changes in the focusing directions when compared to the bulk-wave results.

For comparison, in Figs. 5 and 6 we have plotted the slowness surfaces and focusing patterns for the bulk and surface modes in Fe for different magnitudes of the applied field. One can also study the focusing pattern by changing the frequency at a constant applied field as done in the case of YIG. The results are similar to that of YIG, although the relevant frequencies are very different. In particular, the bulk modes generally display focusing into eight directions, while the surface modes show weak focusing into two directions.

Up to now, we have concentrated on the surface mode and the first bulk mode. Of course, there are many other bulk modes which also could be excited and which should show focusing. In Fig. 7 we show the slowness surface and the

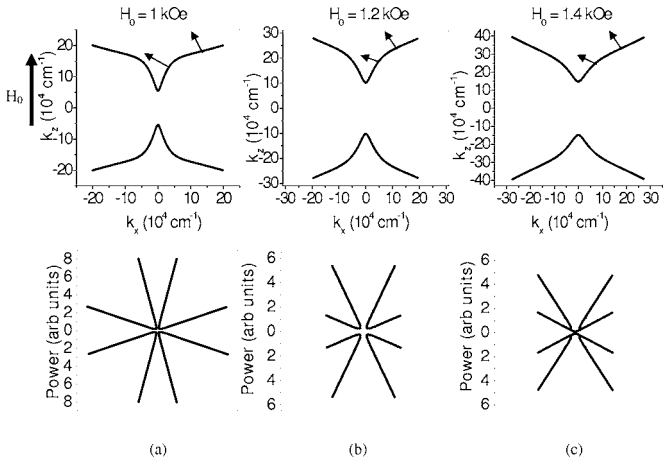

FIG. 5. The upper panel shows the slowness surface and the lower one is the focusing pattern for the lowest bulk mode in Fe at a frequency of 12 GHz with an applied field of (a) 1 kOe, (b) 1.2 kOe, and (c) 1.4 kOe. The arrows on the slowness surfaces show the normals to the slowness surface at some of the points where the curvature is zero.

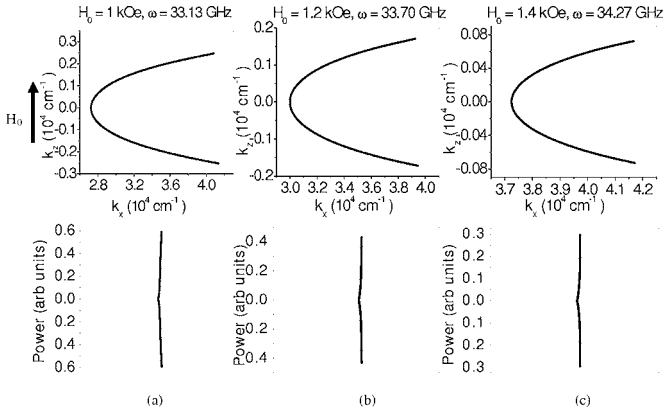

FIG. 6. The upper panel shows the slowness surface and the lower one is the focusing pattern for the surface modes in Fe: (a) H_0=1 kOe, ω=33.13 GHz, (b) H_0=1.2 kOe, ω=33.70 GHz, and (c) H_0=1.4 kOe, ω=34.27 GHz

focusing directions for the first four bulk modes in YIG at different frequencies and with an applied field of 1.2 kOe. We have used a different format to present the data in order to distinguish the modes. Only half of the slowness surface is shown for each mode, and the focusing pattern is shown as a function of angle rather than in a polar plot format. We see in Fig. 7(a) that, for the low frequency case, none of the spin wave modes are truly focused, i.e., there are no caustics, however they all show a substantial increase in power directed in the small range of angles $|\theta| < 40-60°$. At the next frequency of 4.5 GHz, the first bulk mode has a true caustic, but all the remaining bulk modes are not strongly focused. Finally, at the highest frequency shown, 5.2 GHz, all the bulk modes display focusing with true caustics, and the focusing pattern for each mode is different.

IV. THEORY OF DIPOLE-EXCHANGE WAVES

In this section we study the effect of exchange interaction on the focusing pattern. Again, we only outline the calcula-

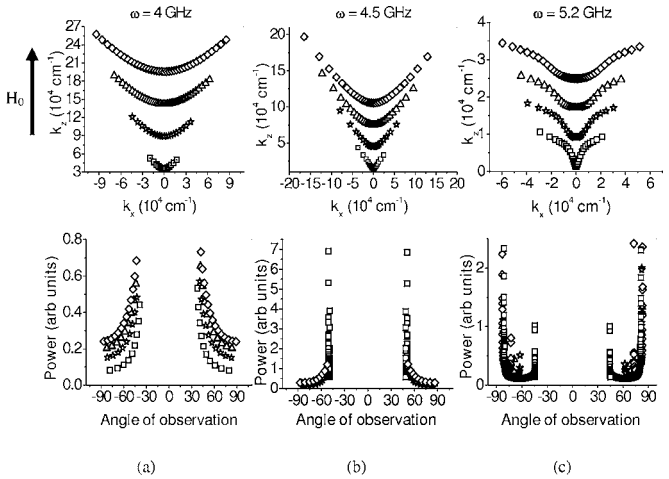

FIG. 7. The upper panel shows the slowness surface and the lower one is the focusing pattern for the different order bulk modes in YIG with an applied field of 1.2 kOe at (a) 4 GHz, (b) 4.5 GHz, and (c) 5.2 GHz.

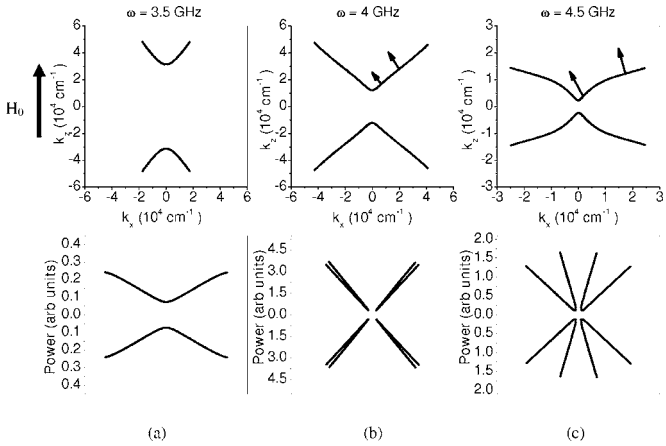

FIG. 8. The upper panel shows the slowness surface and the lower one is the focusing pattern for the lowest bulk mode with exchange effects in YIG with an applied field of 1 kOe at (a) 3.5 GHz, (b) 4 GHz, and (c) 4.5 GHz. The arrows on the slowness surface in (c) show the normals to the slowness surface at some of the points where the curvature is zero. The exchange stiffness $\beta = 5.08 \times 10^{-9}$ G cm^2.

tions. We use the same geometry given in Fig. 1. The calculation includes the usual magnetostatic Maxwell equations along with the equations of motion for the magnetization given as

$$-i\omega \mathbf{m}(\mathbf{r}) = \gamma \mathbf{i}_z \times \{M_s \mathbf{h}_d - [H_0 - \beta \nabla^2]\mathbf{m}\}. \tag{5}$$

Here, $\mathbf{i}_z$ is the unit vector along the z-direction, $\mathbf{h}_d = -\nabla\phi$ is the bulk demagnetizing field, $\mathbf{m} = (m_x, m_y)$ are the oscillating transverse components of the magnetization, H_0 is external field, and the parameter β is exchange stiffness constant. Combining the linearized equations of motion with the magnetostatic form of Maxwell's equations we obtain three equations for the three unknowns, m_x, m_y, and ϕ:

$$\begin{bmatrix} i\omega & \omega_H - D\nabla^2 & \gamma M_s \dfrac{\partial}{\partial y} \\ \omega_H - D\nabla^2 & -i\omega & \gamma M_s \dfrac{\partial}{\partial x} \\ -4\pi \dfrac{\partial}{\partial x} & -4\pi \dfrac{\partial}{\partial y} & \nabla^2 \end{bmatrix} \begin{bmatrix} m_x \\ m_y \\ \phi \end{bmatrix} = 0, \tag{6}$$

where $\omega_H = \gamma H_0$ and $D = \gamma\beta$. As in the case of dipolar waves, one can assume the plane wave solution for magnetization and scalar potential inside the film and obtain a sixth-order polynomial in α. The six roots of the dispersion equation are labeled as α_n, where $n = 1, 2, \ldots, 6$. The solution for ϕ is then a sum over the six partial waves, i.e.,

$$\phi = \sum_{i=1}^{N} \phi_n e^{\alpha_n y} e^{i(q_\parallel \cdot x_\parallel - \omega t)}, \tag{7}$$

and similar expressions exist for m_x and m_y.

To formulate the boundary conditions we express each of the six sets of m_{xn} and m_{yn} in terms of the potential ϕ using Eq. (7). As noted in Sec. II, we use the usual magnetostatic boundary conditions along with the exchange boundary conditions given by

$$\left.\frac{\partial m^\rho(r)}{\partial y} - \xi m^\rho(r)\right|_{y=-d} = 0, \tag{8}$$

$$\left.\frac{\partial m^\rho(r)}{\partial y} - \xi m^\rho(r)\right|_{y=d} = 0, \tag{9}$$

where ρ denotes x or y and ξ is the pinning parameter. In all our calculations, we consider the unpinned condition by choosing $\xi = 0$. Using the above boundary conditions along with the plane wave solution inside and outside the film and after simplification we obtain six homogeneous linear equations for the six unknowns $\phi_1 \ldots \phi_6$ given as

$$\sum_{n=1}^{6} (4\pi m_{yn} - \alpha_n - q_\parallel)\phi_n e^{\alpha_n (d/2)} = 0, \tag{10a}$$

$$\sum_{n=1}^{6} (4\pi m_{yn} - \alpha_n + q_\parallel)\phi_n e^{-\alpha_n (d/2)} = 0, \tag{10b}$$

$$\sum_{n=1}^{6} (\alpha_n - \xi) m_{xn} \phi_n e^{\alpha_n (d/2)} = 0, \tag{10c}$$

$$\sum_{n=1}^{6} (\alpha_n - \xi) m_{xn} \phi_n e^{-\alpha_n (d/2)} = 0, \tag{10d}$$

$$\sum_{n=1}^{6} (\alpha_n - \xi) m_{yn} \phi_n e^{\alpha_n (d/2)} = 0, \tag{10e}$$

$$\sum_{n=1}^{6} (\alpha_n - \xi) m_{yn} \phi_n e^{-\alpha_n (d/2)} = 0. \tag{10f}$$

The condition for Eqs. (10a)–(10f) to have a nonvanishing solution is that the determinant of their coefficients be zero. For a given frequency and applied field we numerically solve the boundary condition matrix to obtain the slowness surface and focusing pattern for both YIG and Fe.

V. EFFECT OF EXCHANGE ON THE FOCUSING PATTERN

We first study the effects of exchange on the focusing pattern of bulk waves. In Fig. 8 we have plotted the slowness surface and corresponding-focusing pattern for the lowest frequency bulk mode including exchange for a 1-μm-thick YIG film at different frequencies. The external field is 1 kOe and the value of $\beta = 5.08 \times 10^{-9}$ G cm^2 is used for exchange stiffness constant. In general the direction of focusing of dipolar-exchange bulk waves are only slightly different to their dipolar counterparts. Even though the directions of the

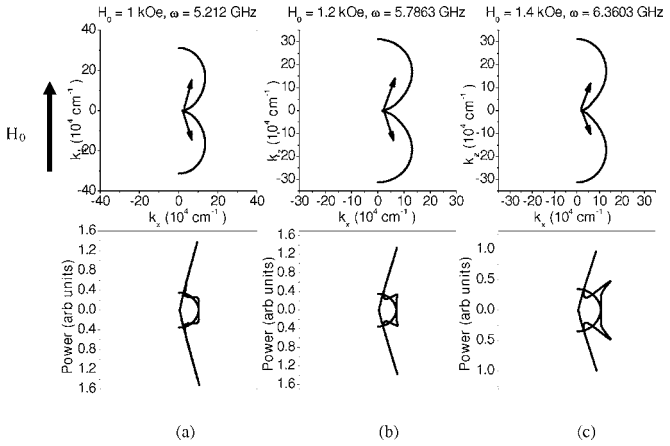

FIG. 9. The upper panel shows the slowness surface and the lower one is the focusing pattern for the surface modes with exchange effects in YIG: (a) $H_0=1$ kOe, $\omega=5.2123$ GHz, (b) $H_0=1.2$ kOe, $\omega=5.7863$ GHz, and (c) $H_0=1.4$ kOe, $\omega=6.3603$ GHz. The arrow on the slowness surfaces show the normals to the slowness surface at some of the points where the curvature is zero. The exchange stiffness $\beta=5.08\times10^{-9}$ G cm^2.

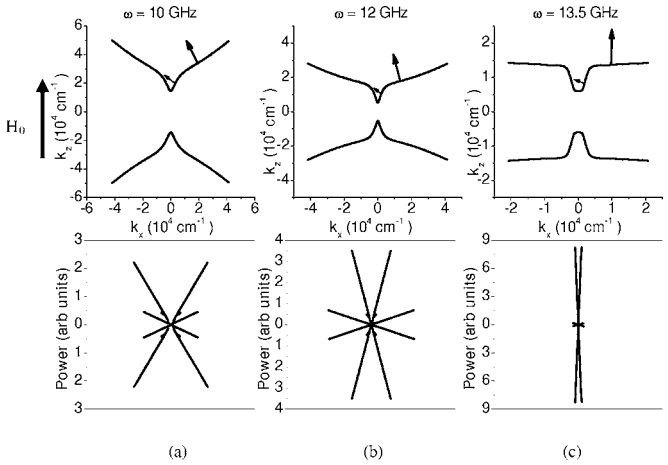

FIG. 10. The upper panel shows the slowness surface and the lower one is the focusing pattern for the lowest bulk mode in Fe with an applied field of 1 kOe at (a) 10 GHz, (b) 12 GHz, and (c) 13.5 GHz. The arrows on the slowness surfaces show the normals to the slowness surface at some of the points where the curvature is zero. The exchange stiffness $\beta=2.2\times10^{-9}$ G cm^2.

focused rays are slightly different, the number of caustics is not affected by the exchange interaction for the bulk waves.

As done in the dipolar case, one can also tune the external field at a constant frequency and study the focusing of dipolar-exchange waves. It is observed that, as the frequency is moved from the top of the bulk frequency band (in the absence of exchange) by changing the external field, the number of true caustics decreases. Also, one can observe that for the parameters considered here, the differences between the focusing patterns for bulk modes calculated with and without exchange are relatively minimal.

The focusing behavior of the surface modes is shown in Fig. 9. Once again, we study the slowness surface and focusing pattern of surface modes on the upper surface of the film. The slowness patterns in Fig. 9 appear to be very different from those in Fig. 4, however we note the scale is quite different. For small wave vectors, on the order of what is seen in Fig. 4, one finds that the two patterns match very closely. The difference is that the slowness surface is restricted to small wave vectors in the dipole-only case. In fact, as the propagation angle gets closer to the direction of the applied field, the surface mode intersects with the upper frequency bound of the bulk band and disappears for the pure dipolar case. When dipole-exchange modes are considered, the bulk band of the dipole-only case has no upper frequency bound and can now range over much larger wave vectors.

The general shape of the slowness surface in Fig. 9 may be understood by the following argument. In the exchange-only limit, the slowness surface would be a circle, with the frequency given by the exchange field; $\omega=Dq_{\parallel}^2$. This circle, of course, must be modified in order to account for the dipolar fields. For propagation perpendicular to the external field, the dipolar field is largest. In order to keep the frequency constant the exchange contribution must be decreased, i.e., the wave vector must be decreased, and the slowness surface is indented at that point.

We now find that the dipole-exchange surface modes are as strongly focused as the bulk waves. In Fig. 9(a) one finds that the curvature of the slowness surface changes sign at couple of points and hence there is true focusing of energy into a caustic. Figures 9(b) and 9(c) show the same effect at different frequency and field where the energy is again focused into true caustics but at different directions.The focusing of both the bulk and surface waves is tunable with the applied field for dipole-exchange waves as was seen earlier in the dipole-only case.

We have plotted the slowness surface and the focusing patterns for the dipole-exchange bulk and surface modes in Fe for different fields and frequencies in Figs. 10–12 for comparison to earlier results without exchange. The exchange stiffness constant for Fe is 2.2×10^{-9}G cm^2. The be-

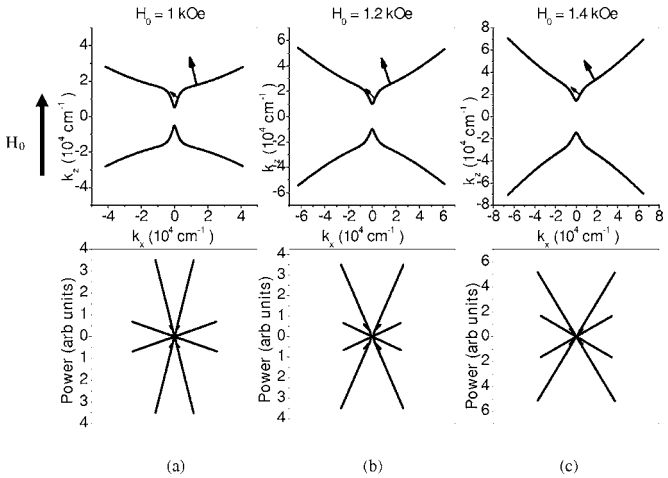

FIG. 11. The upper panel shows the slowness surface and the lower one is the focusing pattern for the lowest bulk mode in Fe at a frequency of 12 GHz with an applied field of (a) 1 kOe, (b) 1.2 kOe, and (c) 1.4 kOe. The arrows on the slowness surfaces show the normals to the slowness surface at some of the points where the curvature is zero. The exchange stiffness $\beta=2.2\times10^{-9}$ G cm^2.

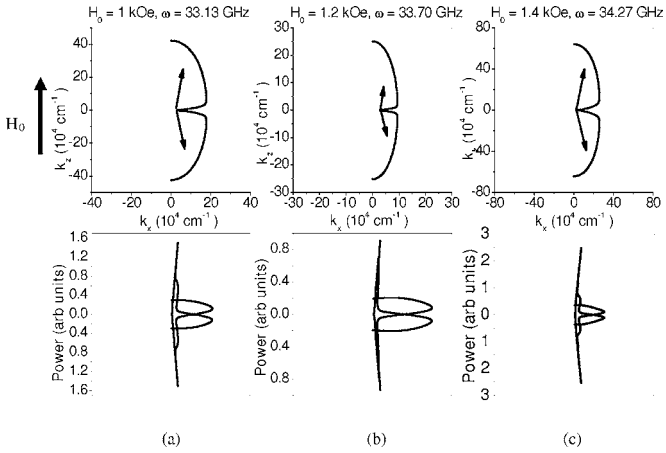

FIG. 12. The upper panel shows the slowness surface and the lower one is the focusing pattern for the surface modes in Fe: (a) H_0=1 kOe, ω=33.13 GHz, (b) H_0=1.2 kOe, ω=33.70 GHz, and (c) H_0=1.4 kOe, ω=34.27 GHz. The arrows on the slowness surfaces show the normals to the slowness surface at some of the points where the curvature is zero. The exchange stiffness β=2.2 $\times 10^{-9}$ G cm^2.

havior of bulk and surface modes are similar to that of YIG. Figures 10 and 11 show the focusing pattern of the dipole-exchange bulk waves in Fe for different frequencies and fields, respectively. The strength and direction of focusing are different compared to YIG because of the higher frequencies of operation. Figure 12 shows the focusing of surface modes into true caustics compared to their dipolar counterparts. One can also find that the higher order bulk modes in dipole-exchange waves show similar focusing effects to the lowest frequency mode.

VI. CONCLUSIONS AND DISCUSSION

In this paper, we have investigated the focusing of magnetostatic bulk and surface modes of dipolar and dipole-exchange waves in ferromagnetic thin films by considering YIG and Fe as the medium. In the case of dipolar waves, we have carried out our analysis by finding the slowness surface for different modes at different frequencies and magnitudes of applied field by solving the implicit dispersion relation for ferromagnetic thin film. From the slowness surface, we obtained the focusing pattern by numerically evaluating the curvature of the surface at every point on it. The results show that we can obtain substantial focusing of magnetostatic waves in YIG and Fe. Furthermore, the backward volume waves are strongly focused when compared to the surface waves. The number of focusing directions depends on the operating frequency and we obtain eight distinct focusing directions when the frequency is at the top of bulk magnon region. Also, the focusing directions change by changing the magnitude of the applied field. The effect of exchange on the focusing behavior of bulk and surface waves is studied by considering the dipole-exchange waves. We find that the focusing behavior of the bulk waves are not much affected by the exchange, while the surface modes are strongly focused in the case of dipolar-exchange waves in both YIG and Fe.

Experimentally, it should be possible to view the focusing of these magnetostatic waves for example by using a scanning Brillouin light scattering technique.[22] Recent experimental works in this area has focused on nonlinear effects,[22] but there have already been some observations of focusing in magnon propagation on YIG. In particular, we note an experiment where magnetic spin waves at a particular frequency were generated by a stripline above a YIG sample. The spin waves propagated away from the stripline, hit an impurity and showed distinct focusing of energy into two particular directions.[22]

Because different external fields cause the energy to be focused into different directions, we can use this idea to make tunable filters. For example, a particular frequency could be directed to a particular receiver using the focusing effect. Furthermore, at a given field different frequencies are focused in different directions. This could be used to build a device that separates frequencies in the microwave frequency range which could find an application in radar systems, for example. A typical electronic support system analyzes the amplitude and distribution of microwave signals over a range of frequencies by scanning over narrow frequency bands using a tunable bandpass filter. In contrast, the separation of frequencies shown here occurs with a single device and field setting, eliminates the need for tuning.

ACKNOWLEDGMENTS

This work was supported by DOA Grant No. W911NF-04-1-0247 and US ARO Contract No. DAAD19-02-1-0174. The authors would also like to acknowledge helpful discussion with B. Hillebrands.

[1] T. Buchwald, Proc. R. Soc. London, Ser. A **253**, 563 (1959).
[2] B. Taylor, H. J. Maris, and C. Elbaum, Phys. Rev. Lett. **23**, 416 (1969); Phys. Rev. B **3**, 1462 (1971).
[3] P. Taborek and D. Goodstein, Solid State Commun. **33**, 1191 (1980).
[4] V. T. Buchwald, Q. J. Mech. Appl. Math. **14**, 293 (1960); V. T. Buchwald and A. Davis, *ibid.* **16**, 283 (1963).
[5] J. C. Hensel and R. C. Dynes, Phys. Rev. Lett. **43**, 1033 (1979).
[6] G. A. Northrop and J. P. Wolfe, Phys. Rev. B **22**, 6196 (1980).
[7] R. E. Camley and A. A. Maradudin, Phys. Rev. B **27**, 1959 (1983).
[8] L. R. Walker, Phys. Rev. **105**, 390 (1957); J. Appl. Phys. **29**, 318 (1958).
[9] See the review article by L. R. Walker, in *Magnetism*, edited by G. T. Rado and H. Suhl (Academic, New York, 1963), p. 299.
[10] R. W. Damon and J. R. Eshbach, J. Phys. Chem. Solids **19**, 308 (1961).
[11] M. Sparks, Phys. Rev. B **1**, 3831 (1970).

[12] B. E. Storey, A. O. Tooke, A. P. Cracknell, and J. A. Przystawa, J. Phys. C **10**, 875 (1977).
[13] P. H. Bryant, J. F. Smyth, S. Schultz, and D. R. Fredkin, Phys. Rev. B **47**, 11255 (1993).
[14] R. D. McMichael and M. D. Stiles, J. Appl. Phys. **97**, 10J901 (2005).
[15] K. Y. Guslienko, R. W. Chantrell, and A. N. Slavin, Phys. Rev. B **68**, 024422 (2003).
[16] G. Leaf, H. Kaper, M. Yan, V. Novosad, P. Vavassori, R. E. Camley, and M. Grimsditch, Phys. Rev. Lett. **96**, 017201 (2006).
[17] L. Giovannini, F. Montoncello, F. Nizzoli, G. Gubbiotti, G. Carlotti, T. Okuno, T. Shinjo, and M. Grimsditch, Phys. Rev. B **70**, 172404 (2004).
[18] M. G. Cottam and D. R. Tilley, *Introduction to Surface and Superlattice Excitations* (Cambridge University Press, Cambridge, 1989).
[19] R. E. Camley and D. L. Mills, J. Appl. Phys. **82**, 3058 (1997).
[20] R. J. Astalos and R. E. Camley, J. Appl. Phys. **83**, 3744 (1998).
[21] R. L. Stamps and R. E. Camley, Phys. Rev. B **31**, 4924 (1985).
[22] O. Büttner, M. Bauer, S. O. Demokritov, B. Hillebrands, Yu. S. Kivshar, V. Grimalsky, Yu. Rapoport, and A. N. Slavin, Phys. Rev. B **61**, 11576 (2000).